

UVM ScholarWorks

Knee articular cartilage quantitative MRI reliability and left-to-right and visit-to-visit repeatability in healthy subjects under compressive loading

Item Type	thesis;article
Authors	Borah, Andrew
Download date	2026-05-08 14:27:30
Link to Item	https://hdl.handle.net/20.500.14849/3842

KNEE ARTICULAR CARTILAGE QUANTITATIVE MRI RELIABILITY AND LEFT-
TO-RIGHT AND VISIT-TO-VISIT REPEATABILITY IN HEALTHY SUBJECTS
UNDER COMPRESSIVE LOAD

A Thesis Presented

by

Andrew Borah

to

The Faculty of the Graduate College

of

The University of Vermont

In Partial Fulfillment of the Requirements
For the Degree of Master of Science
Specializing in Biomedical Engineering

May, 2024

Defense Date March 15th, 2024
Thesis Examination Committee:

Bruce Beynon Ph.D., Advisor
Mat Failla Ph.D., Chairperson
Niccolo Fiorentino Ph.D.
Tim Tourville Ph.D.
Holger Hoock, DPhil, Dean of the Graduate College

Abstract

Purpose: Quantitative magnetic resonance imaging (qMRI) metrics, including T1 ρ and T2*, exhibit considerable promise as image-based biomarkers to monitor the progression of osteoarthritis and post traumatic osteoarthritis. The potential for tracking disease progression utilizing these metrics may be further enhanced with the joint under loaded conditions, as an abnormal response to loading may contribute to cartilage degeneration. Reliability and repeatability studies for T1 ρ and T2* measurements have yielded variable results, compared surgical to non- surgical knees, employed diverse sample regions of interest, and acquired images under traditional non-weight bearing knee conditions. The purposes of this study are to quantify side-to-side and visit-to-visit repeatability of T1 ρ and T2* in healthy subjects in both unloaded and loaded cartilage, and to evaluate how ROI selection affects the variability of relaxation times.

Materials and Methods: Ten healthy participants (6 female, 4 male) underwent bilateral qMRI over two visits (7 \pm 3 days apart) on the same Philips 3T MR system. After scanning without load, each knee was imaged with a 40% body-weight external load applied to the knee using a custom-built MRI-compatible loading device. Interclass correlation coefficients (ICC) and ANOVA with statistical significance of $p < .05$ were used to analyze left-to-right and visit-to-visit differences.

Results: Across all ROIs, T1 ρ ICCs ranged from 0.13-0.77, while T2* ICCs ranged from 0.22-0.82. Across all ROIs, left-to-right mean differences were 2.6 ms for T1 ρ and 1.9 ms for T2* and visit-to-visit, mean differences were .003 ms for T1 ρ and -0.2 ms for T2*.

Conclusion: Quantitative MRI has fair repeatability, with tibial cartilage generally better than femoral cartilage, but may be affected by ROI selection and subject to a limb sidedness bias that needs further investigation.

Table Of Contents

Introduction.....	1
Methods	3
Results.....	10
Discussion.....	15
References.....	21
Appendix A- Supplemental Materials.....	24

Introduction

Quantitative magnetic resonance imaging (qMRI) measures have been shown to correlate with articular cartilage matrix component composition (1). For example, T1 ρ relaxation times are negatively correlated with cartilage proteoglycan content, and positively correlated with water content (2), while T2* relaxation times are correlated with changes in cartilage collagen matrix orientation (3). Indeed, qMRI measures have shown promise as potential image-based biomarkers for studying the early changes in cartilage and meniscus matrix composition associated with primary osteoarthritis (OA) progression. Similarly, there is evidence that qMRI changes may be associated with the onset and progression of post traumatic osteoarthritis (PTOA) that precede structural changes about the knee (4-6). It is thought that qMRI can be applied to quantify early alterations in metabolism of articular cartilage and meniscus matrix (i.e. the synthesis and cleavage of matrix components that occurs early in the PTOA and OA disease process) prior to the changes that are observed with the use of conventional clinical MRI.

Abnormal loading of the articular cartilage and meniscus about the knee has been hypothesized to lead to cartilage degeneration (8). Consequently, an understanding of how load affects cartilage matrix composition may provide valuable insight into the pathogenesis and progression of OA and PTOA (9). Application of compressive loads to the knee joint that replicates body weight loading can be accomplished by having the subject stand upright in an open bore MRI, or with a device that applies compressive loading to the knee with the use of traditional closed bore MRI. With both approaches MRI scanning parameters are usually chosen with consideration of minimizing

acquisition time due to load application, as subject comfort and tolerance to external load and the subsequent motion artifact that may occur, must be considered. Consequently, shorter scans may suffer from reduced resolution and produce noisier, more variable qMRI metrics. It is also important to note that scans are performed one knee at a time to take advantage of specialized coils with multiple channels. While this reduces time for the first knee scanned, the knee that is scanned second experiences longer times of non-weightbearing, possibly introducing bias into the results as cartilage is a viscoelastic tissue depends on the temporal history of loading/ unloading. It is therefore imperative to understand the reliability of these scans in both knees in both loaded and unloaded conditions.

While T1 ρ measures, without application of an external load, have been shown to be reliable and repeatable (10), very little is known about the reliability and repeatability of T2* acquisitions, which is thought to be relatively insensitive to the magic angle effect. Further, limited information has been published on the reliability and repeatability of both sequences when the knee is supporting load. Another potential confounding factor is the high amount of variability associated with methods that have been used to acquire qMRI scans (10). In addition, there does not appear to be a common approach for the methods used to post-process the T1 ρ and T2* data including segmentation, registration, and decay curve fitting. Moreover, several different methods for defining the regions of interest (ROIs) have been used. For example, one approach has been to analyze only select slices (11), while another approach has been to analyze the entire cartilage volume to generate relaxation times. New evidence suggests that a laminar analysis that considers deep and superficial articular cartilage separately may provide different qMRI measures,

with $T2^*$ being particularly sensitive to changes in the deep zone of cartilage (12). An improved understanding of how the ROI selection affects the reliability of qMRI measurements would be beneficial, especially considering most research reports only one uniquely defined ROI in the results.

Reliability and repeatability of $T1\rho$ and $T2^*$ relaxation times should be analyzed and understood in healthy subjects as these data are essential for determining if the early changes in cartilage matrix that are associated with PTOA can be quantified by these qMRI measurement techniques. This information is important for interpreting changes of relaxation times acquired from subjects that have suffered knee trauma or are at increased risk for PTOA using both between knee study designs, (i.e., using the healthy knee as a control), and within-knee longitudinal study designs. In order to determine the magnitude of qMRI relaxation times that are pathological and attributed to a disease process such as PTOA, a necessary first step is to establish the variance within the measure itself (e.g., location in relation to $B0$ using phantoms), as well as normal variance in subjects with healthy knees. Therefore, the purposes of this study are to quantify visit-to-visit reliability and left-to-right knee differences of $T1\rho$ and $T2^*$ metrics in healthy subjects with the knee in unloaded and loaded conditions, and to determine how ROI selection affects the variability of the qMRI relaxation times. We hypothesized there will be no effect of side and visit on qMRI metrics obtained with the knee unloaded and loaded, and that the visit-to-visit ICCs will improve with larger ROIs due to incorporation of more voxels.

Methods

Subjects and Study Design

Ten participants (6 female, 4 male) with no known history of lower extremity injury were recruited and provided written consent prior to participating in this university IRB-approved study. Subject demographics were: age (\pm SD) 23 (\pm 2.4) yr, weight 77.1 (\pm 13.2) kg, height 1.75 (\pm 0.08) m. Data were collected at two visits, separated by a mean of 7 (\pm 3) days. Each visit was comprised of a 15-minute off-loading period during which the subject sat in a wheelchair with their knees unloaded, followed by T1 ρ and T2* acquisition with the left leg unloaded, T1 ρ and T2* acquisition with the left leg loaded, and finally T1 ρ and T2* acquisition with the right leg unloaded and then loaded. This protocol was repeated on visit 2 (Fig. 1).

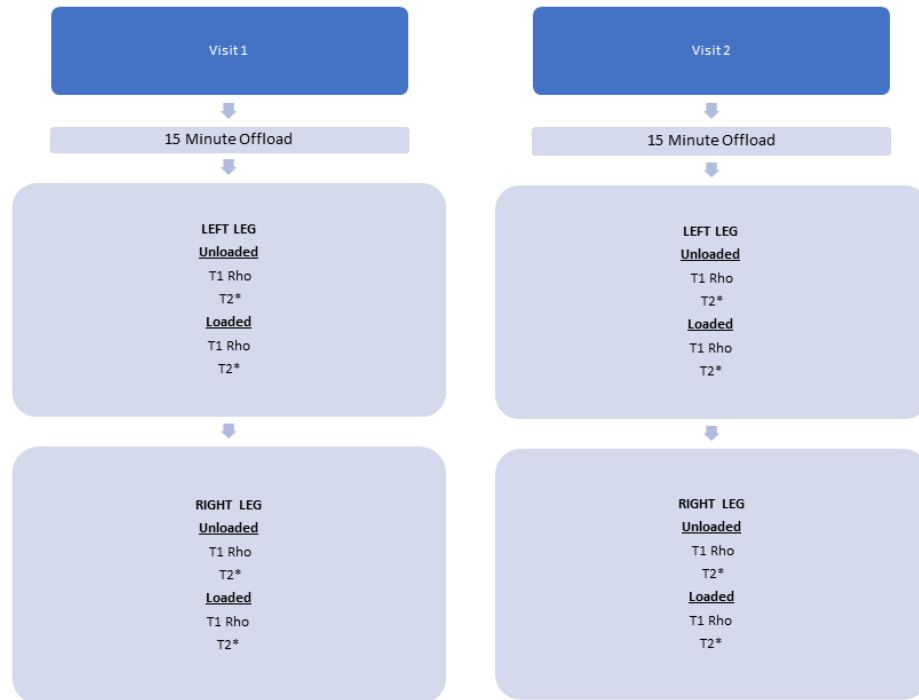


Figure 1: Study visit structure. Depicts scanning order moving from top to bottom over both visits.

MRI Acquisition

During each visit bilateral MRIs of the participants knees were acquired on the same Philips 3T MR system (Achieva, Philips Healthcare, Best, The Netherlands) with a 16 channel transmit-receive radiofrequency knee coil. A 40% body-weight load was applied to the plantar aspect of the subjects' foot during loaded scans using a custom-built MRI-compatible loading device described by Ramsdell et al. (13). (See Supplemental Figures 1 and 2 (Figs. S1 and S2) for an illustration of loading device.) The same investigators positioned the subject in the scanner and carried out the acquisitions for all subjects at both visits. Subject alignment was recorded to replicate positioning of their legs between visits. Alignment measures taken included adjusting greater trochanter and lateral malleolus height to ensure full knee extension by orienting them level to the lateral epicondyle of the knee, hip abduction/adduction, ankle inversion/eversion, and hip internal/external rotation positions were all recorded and duplicated between visits.

A single three-dimensional (3D) acquisition in the sagittal plane comprised of four spin lock times of 0, 10, 40, and 80 ms at a spin lock frequency of 500 Hz was used to collect the data necessary to calculate $T1\rho$ relaxation times (Table 1A). This protocol utilized a prepared angle modulated partitioned k-space spoiled gradient echo snapshots (3D MAPSS) sequence (14). Acquisitions were reconstructed to a voxel size of $0.49 \times 0.49 \times 1.5 \text{ mm}^3$ over a field of view of $250 \times 141 \times 96 \text{ mm}^3$.

The $T2^*$ sequence was acquired using a 3D gradient echo sequence with spiral-out k-space and stack of spirals trajectory sampling strategies (Table 1B). Multiple individual acquisitions for a total of five echo times (0.42, 1.0, 5.0, 15.0, and 30.0 ms) in the sagittal plane were acquired and used to calculate $T2^*$ relaxation times. Images were

reconstructed to a voxel size of $0.44 \times 0.44 \times 2 \text{ mm}^3$ over a field of view of $140 \times 140 \times 96 \text{ mm}^3$.

Table 1: Three-dimensional (3D) T1 ρ (A) and T2* (B) scanning parameter values.

(A) 3D T1ρ imaging		(B) 3D T2* imaging	
Parameter	Value	Parameter	Value
Field-of-view (mm ³)	250 x 141 x 96	Field-of-view (mm ³)	140 x 140 x 96
Acquired matrix size	500 x 281 x 32	Acquired matrix size	232 x 232 x 24
Image orientation	Sagittal	Image orientation	Sagittal
Reconstructed matrix size	512 x 512 x 64	Reconstructed matrix size	320 x 320 x 48
Reconstructed voxel size (mm ³)	0.49 x 0.49 x 1.5	Reconstructed voxel size (mm ³)	0.44 x 0.44 x 2.00
Time of recovery (ms)	2150	Echo times (ms)	0.42, 1, 5, 15, 30
Spin-lock times (ms)	0, 10, 40, 80	Repetition time (ms)	50
Echo time (ms)	5.1	Flip angle (°)	8
Repetition time (ms)	10	Spiral acquisition window (ms)	2.9
Flip angle maximum (°)	70	Number of spiral interleaves	93
Acquisition time	9 min 11 s	Fat suppression	SPIR
Bandwidth per pixel (Hz/pix)	287.4	Acquisition duration	9 min 19 s
TFE factor	92	B ₀ shimming	PB-volume
Spin-lock frequency (Hz)	500		
Compress Sensing factor	3.2		
TFE profile order	Low-high		
TFE turbo direction	Radial		
Fat suppression	ProSet-1331		

Post-Processing

Tibial and femoral subchondral bone and articular cartilage surfaces were segmented manually in the sagittal plane, on the 0 ms spin lock time for T1 ρ , and the 5.0 ms echo time for T2*, using a Cintiq interactive pen display and touch tablet (Wacom, Toyonodai, Kazo-shi, Saitama Japan) and OsiriX medical imaging software (Bernex, Switzerland) (15). Segmentations were imported into custom MATLAB (The MathWorks Inc., Natick, MA) software for post-processing (16). Every acquisition's spin lock (T1 ρ) / echo (T2*) times were registered together using a 3D rigid body translation and rotation with ELASTIX (17-19). Image volume registrations were performed to the corresponding spin lock / echo time on which segmentations were done for each respective scan. Three scans were omitted from analysis due to poor image volume registrations.

Several ROIs of differing size were defined for analysis utilizing the articular cartilage segmentations (Fig. 2). The largest ROI was the full tibial and femoral cartilage ROIs combined, including both medial and lateral compartments (Fig. 2B). (The trochlear cartilage on the femur was excluded to match its exclusion when split into medial and lateral compartments.) Next, the femoral cartilage ROI included both medial

and lateral compartments (Fig. 2C), as did the tibial cartilage ROI (Fig. 2D). Then, each bone and compartment were isolated for the lateral femoral cartilage (Fig. 2E), medial femoral cartilage (Fig. 2F), lateral tibial cartilage (Fig. 2G), and medial tibial cartilage (Fig. 2H). The smallest ROI was a 6 mm radius cylinder, referred to as a “plug”, that was defined by the centroid of the tibiofemoral contact area with the long axis of the cylinder aligned with the inferior-superior directed axis of the imaging volume (13). A single plug was generated for both the lateral and medial compartments that included both tibial and femoral articular cartilage. The articular cartilage voxels contained in the plugs were split into lateral femoral (Fig. 2I), medial femoral (Fig. 2J), lateral tibial (Fig. 2K), and medial tibial (Fig. 2L) cartilage. Last, each of the plugs and individual bone-compartments (i.e., Fig. 2E-L) was also further split into deep (50 percent of the cartilage adjacent to the subchondral bone) and superficial (50 percent of the cartilage adjacent to the surface) laminar layers.

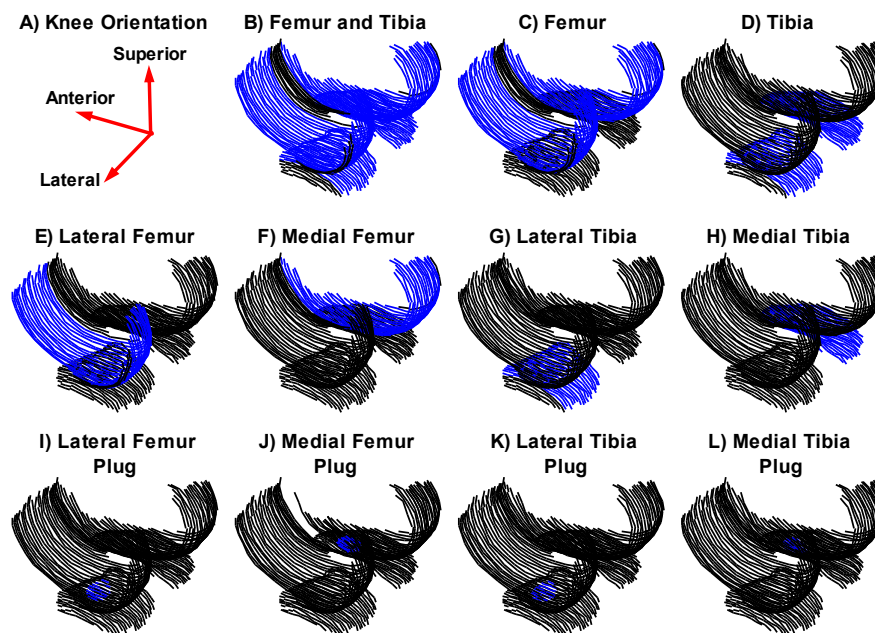


Figure 2: Articular cartilage segmentations in each region of interest (ROI) illustrated in blue, with ROI size decreasing from top to bottom rows. The top two rows show full-surface ROIs, and the bottom row shows 6 mm plug ROIs. The 6 mm plug ROIs were formed from a cylindrical “plug” at the centroid of the tibiofemoral contact area in each compartment with a radius of 6 mm. Additional ROIs with the articular cartilage divided into deep and superficial layers are not shown.

A mono-exponential fit was applied to each voxel within an ROI to calculate relaxation times using the Levenberg-Marquardt algorithm (20,21) for both T1 ρ and T2*. The average of all included pixel relaxation times within a ROI was calculated and used to generate an overall relaxation time for each ROI.

Statistical Analysis

Interclass correlation coefficients (ICCs) for mean relaxation times in each ROI were calculated, using both between-leg and between-visit variance components in the error term of the ICC formula. These ICCs were calculated for T1 ρ and T2* relaxation times for both the unloaded and loaded conditions for each ROI.

Descriptive statistics (means/standard deviations) for T1 ρ and T2* by knee (left and right) and by visit (time points 1 and 2) were generated for both the unloaded and loaded conditions for each ROI. Comparisons of mean T1 ρ and mean T2* relaxation times between left and right knees and between visits, for both the unloaded and loaded conditions of each ROI, were done using mixed model repeated measures analyses of variance. For these models, the random effect was subject, and the repeated measures, and fixed effects, were leg and visit, correspondingly. All statistical analyses were done using SAS version 9.4 statistical analysis software (SAS Institute, Inc., Cary, NC, USA). Statistical significance level alpha was set *a priori* to 0.05.

Results

ICC Analyses for Comparison Between Visits 1 and 2:

T1 ρ

Analysis of the visit-to visit T1 ρ relaxation times for the unloaded femur and tibia ROI (picture in Fig. 2B) produced an ICC value that was 0.55, and the loaded condition was 0.69 (Fig. 3). The unloaded tibia had ICC values that ranged from 0.31 to 0.62 for the combined and individual compartments (Fig. 2D, G/H) and from 0.31 to 0.72 for the plugs (Fig. 2K/L). The tibia in the loaded condition had ICC values that ranged from 0.46 to 0.77 for the combined and individual compartments and from 0.42 to 0.76 for the plugs. For the femur, in the unloaded condition, ICC values ranged from 0.31 to 0.39 for the combined and individual compartments (Fig. 2C, E/F) and from 0.13 to 0.36 for the plugs (Fig. 2I/J). The loaded femur ICC values ranged from 0.29 to 0.75 for the combined and individual compartments and between 0.22 and 0.41 for the plugs.

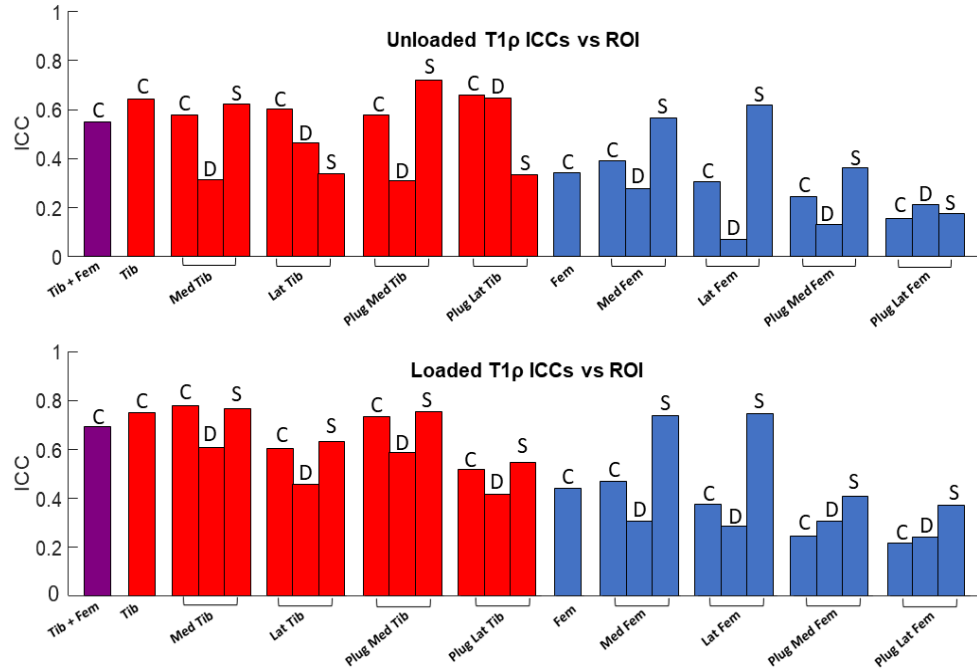


Figure 3: T1 ρ intraclass correlation coefficients (ICCs) including left-right leg variance for unloaded and 40% body weight loaded conditions. Letters on top of the bars signify the cartilage layer: “C” for the combined (deep and superficial) cartilage layers, “D” for the deep cartilage layer, and “S” for the superficial cartilage. Tib: tibial cartilage. Fem: femoral cartilage. Med: medial. Lat: lateral.

T2*

Analysis of the visit-to-visit T2* relaxation times for the femur and tibia ROI resulted in an ICC value of 0.67 for the unloaded condition and 0.57 when loaded (Fig. 4). The unloaded tibia had ICC values that ranged from 0.38 to 0.78 for the combined and individual compartments and 0.43 to 0.78 for the plugs. With the tibia in the loaded condition, ICC values ranged from 0.31 to 0.62 for the combined and individual compartments and 0.43 to 0.71 for the plugs. The unloaded femur ranged between 0.41 and 0.69 for the combined and individual compartments and 0.23 to 0.82 for the plugs.

Finally, the ICCs associated with the loaded femur ranged from 0.38 to 0.48 for the combined and individual compartments and from 0.22 to 0.70 for the plugs.

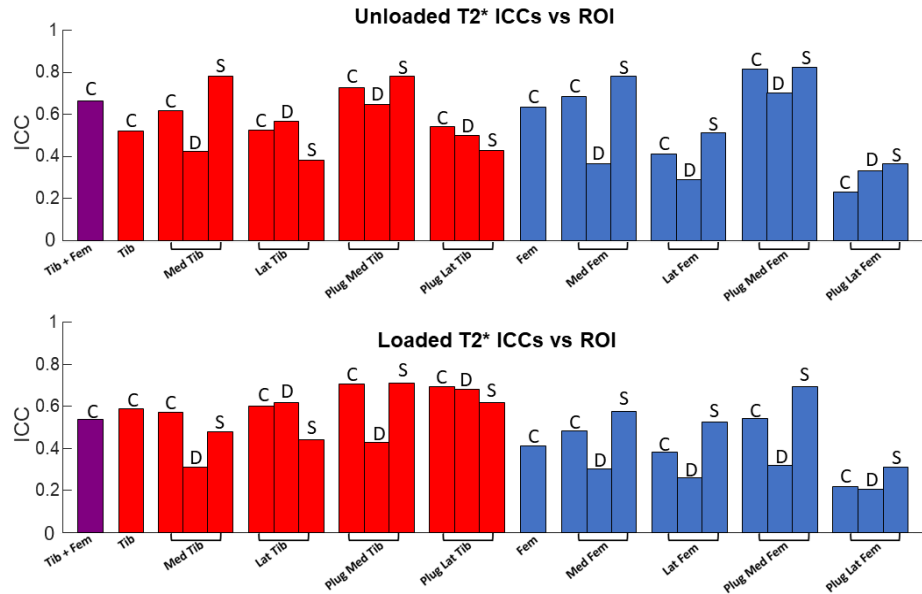


Figure 4: T2* intraclass correlation coefficients (ICCs) including left-right leg variance for unloaded and 40% body weight loaded conditions. Letters on top of the bars signify the cartilage layer: “C” for the combined (deep and superficial) cartilage layers, “D” for the deep cartilage layer, and “S” for the superficial cartilage. Tib: tibial cartilage. Fem: femoral cartilage. Med: medial. Lat: lateral.

Mixed Model Repeated Measures Analyses of Variance for Comparisons Between Right and Left Knees and Visits 1 and 2:

T1ρ

For T1ρ full volume (femur + tibia, femur, and tibia, Fig. 2B-D), five of the six comparisons of means between left and right knees for the combined layer ROIs across both unloaded and loaded conditions were statistically significant (Table 2: p-values ranged between 0.0001 and 0.045), with only the result for the loaded tibia being non-significant. The mean relaxation times for the right knee were consistently greater than

the left knee for each ROI comparison. For ROIs by layer (deep/superficial, Fig. 2E-H), six of the eight comparisons of mean T1 ρ full volume relaxation times between right and left knees for the unloaded condition were significantly different (p-values ranged between 0.0001 and 0.04), while three of the eight comparisons between knees for the loaded condition were significantly different (p-values ranged between 0.001 and 0.02). The right knee mean values were consistently greater than the left knee for each of these significant differences. For the T1 ρ plug ROIs (Fig. 2I-L), four of the eight comparisons of mean relaxation times between knees for combined layer ROIs across both unloaded and loaded conditions were significantly different (p-values ranged between 0.001 and 0.046), with the right knee mean relaxation time values consistently greater than the left knee for each comparison. For ROIs by layer (deep/superficial, Fig. 2I-L), six of the eight comparisons of mean T1 ρ plug relaxation times between knees for the unloaded condition were significantly different (p-values ranged between 0.001 and 0.04), while three of the eight comparisons for the loaded condition were significantly different (p-values ranged between 0.001 and 0.01). Again, the mean relaxation times associated with the right knee were consistently greater compared to the left knee for each of the significant findings. There were no significant differences in mean T1 ρ full volume segmentation or T1 ρ plug relaxation times between visits for any ROI across unloaded and loaded conditions. All results for comparisons between visits, and descriptive statistics by visit, for these measures are presented in the supplemental text (Tables S1 and S2).

T2*

For T2* full volume segmentations (femur + tibia, femur, and tibia, Fig. 2B-D), four of the six comparisons of mean relaxation times between legs for combined layer ROIs across both unloaded and loaded conditions were statistically significant (p-values ranged between 0.002 and 0.01), with only the results for unloaded femur and loaded tibia being non-significant, and with greater right leg mean values compared to the left for each comparison (Table 3). For ROIs by layer (deep/superficial, Fig. 2E-H), three of the eight comparisons of mean T2* full volume segmentations between legs for the unloaded condition were significantly different (p-values ranged between 0.004 and 0.03), while only one of the eight comparisons for the loaded condition was significant (Lateral Femur Deep, $p = 0.002$). There were greater right leg mean relaxation values for each of these significant differences. For T2* plug (Fig. 2I-L), five of the eight comparisons of means between legs for combined layer ROIs across both unloaded and loaded conditions were significant (p-values ranged between 0.02 and 0.03), with greater right knee mean relaxation time values than the left in each case. For ROIs by layer (deep/superficial, Fig. 2I-L), five of the eight comparisons of mean T2* plug between legs for the unloaded condition were significantly different (p-values ranged between 0.03 and 0.04), while three of the eight comparisons for the loaded condition were significant (p-values ranged between 0.02 and 0.04). The right leg mean relaxation values were greater than the left for each of these significant differences. There was only one significant difference in mean T2* plug between visits, with greater visit 1 mean relaxation times compared to visit 2 for the medial tibia ROI in the unloaded condition ($p = 0.02$). There were no significant differences in mean T2* full volume segmentations between visits. All analysis results for comparisons between visits, and descriptive

statistics by visit, for these measures are presented in the supplemental text (Tables S3 and S4).

Discussion

ICC analyses revealed a relatively high amount of variation between visits 1 and 2 for T1 ρ and T2* relaxation times, and this occurred between ROIs, as well as within an ROI when it was further divided into smaller regions. Further, many of the ICC values between visits associated with the tibia ROIs were considered fair or good, while the values for the femur were considered to have poor or fair reliability. This finding indicates that the cartilage associated with each bone should be analyzed separately and not as a combined ROI. The ROI size did not seem to have a direct connection to the ICC value as we initially hypothesized. Similarly, we observed a side-to-side difference in healthy knees that we did not hypothesize. On the other hand, the visit-to-visit differences were low and not significantly different aside from one ROI. Our study was unique in studying the reliability and repeatability in the deep and superficial layers separately, and this revealed the relaxation times associated with the superficial region of cartilage could be measured with more reliability than the deep regions. We also observed that the ICC values between visits for the loaded condition were more reliable than the unloaded condition, and this may have been produced by improved control of knee position and reduced movement of the subjects during scanning while in the loading device.

For T1 ρ in general, the tibia showed higher ICCs than the femur across the array of different ROIs (Fig. 3), with an average of 0.60 (tibia) compared to 0.33 (femur). The loaded condition also tended to be associated with higher ICCs with an average of 0.52 in

the loaded condition and 0.39 in the unloaded condition. Looking specifically at the laminar analysis, the superficial zone showed better ICCs than the deep zone with average values of 0.54 in the superficial layer and 0.35 in the deep layer. In general, T2* showed higher ICCs in the tibia when compared with the femur (Fig. 4), with an average of 0.58 for the tibia and 0.47 for the femur. This result agrees with the results found by Zhang et al. who also observed higher ICCs in the tibia compared to the femur (22). Conversely the T2* showed slightly higher ICCs in the unloaded condition (averaging 0.56) when compared to the loaded condition (averaging 0.49). Lastly, as with T1 ρ , the T2* relaxation times showed higher reliability in the superficial layer, averaging 0.58 compared to 0.44 in the deep layer. Welsch et al. (23) suggests that T2* reliability is high in the patella. While other studies have shown higher reliability than the current MRI reliability study overall (10), we have shown that ROI selection plays a role in reliability. To our knowledge, this is the first report of reliability on normal knee articular cartilage T2* while the joint is subjected to compressive loading.

The left-to-right knee differences in T1 ρ and T2* relaxation times observed in this study contrasted with the small visit-to-visit differences in relaxation times. These small differences in relaxation values over time have also been observed in T1 ρ relaxation times by Lartey et al. (24). It is also important for us to highlight for both qMRI acquisitions the relaxation times obtained from the right knee were consistently greater than the left knee. The magnitude of some of the left-to-right knee differences were similar to the magnitude of differences between normal and diseased knees associated with the onset and progression of PTOA (25). This finding provides evidence that there may be a limb sidedness effect, and therefore within knee cohort study designs, such as

longitudinal studies, may be more appropriate for investigations that use qMRI measurements. To further complicate the situation, Xie et al. highlighted small changes in inter and intra site relaxation times in phantoms (26). This work indicates that relaxation times may be affected by both position of the limb in the scanner and scanner manufacturer. Across all ROIs the mean differences in T1 ρ relaxation times were 2.6 ms for left-to-right knee and 0.003 ms for visit-to-visit comparisons, while the differences in T2* relaxation times were 1.9 ms for left-to-right knee and -0.2 ms for visit-to-visit comparisons. These findings suggests that leg scanning order and offloading time may play an important role in qMRI relaxation times and should be considered and either controlled when creating study designs or considered in the statistical analysis. While the left-to-right differences were statistically significant, the percent change for the left to right differences across all ROIs were relatively small at 6.8% for T1 ρ and 6.5% for T2*. The visit-to-visit differences were even smaller at .007% for T1 ρ and .68% for T2*. These differences are critical to understanding the limits of qMRI measures when comparing knees over time or to the contralateral side.

Prior to initiating the current study, we conducted a laboratory-based (i.e., without MRI) study to ensure consistent load application withing a 12-minute trial, between three trials during the same visit, between three visits on different days, between two examiners, and across ten participants. This work is presented in the supplemental text. (Participants provided written informed consent prior to participation in the IRB-approved study.) We showed the ability to consistently apply an axial compressive load over time (see example force vs. time plot in Fig. S5) and between examiners, trials, and visits using a six degree-of-freedom force sensor placed at the foot pedal and in line with

the heel. The mean force for a trial was never greater than 0.02% BW between examiners, trials, and visits, with standard deviations between 1.0% and 1.1% BW across examiners, trials, and visits. This worked confirmed there were no appreciable off-axis loads or moments utilizing this loading device. This prior study used a 50% body weight load at 12-minute application intervals based on the work of Wang et al. (27). During this laboratory-based study, 20% of subjects showed limited tolerance to the load. Consequently, we reduced the load to 40% body weight for the study described herein. We also measured the motion of a marker affixed to the patella by taking photographs every two minutes, and we found the ~60% of the movement in the superior direction occurred in the first two minutes, with an average of 0.8 mm subsequently in the 2-12 minutes range. Therefore, we felt it was important to keep the total time in loading device to the 12-minute interval due to subject tolerance, and we started scanning after two minutes of applying load, resulting in a ~10 minute scan. We then set the scanning parameters to acquire the best results in that time frame for the results described herein.

We chose a 15-minute offloading time interval prior to acquisition of qMRI data based on the protocol described by Van Ginckel et al. (28). The protocol we used consistently acquired qMRI data from the left knee first followed by the right knee, as this is the standard protocol for our imaging center. Left knee acquisitions were initiated, on average 20.1 (\pm 5.7) minutes after the start of offloading and this was followed by the right knee acquisition that were initiated an average of 94.6 (\pm 9.6) minutes after the start of offloading. It is possible that the mechanism that produced the left-to-right knee differences in relaxation times is a result of this offloading time difference between knees. Alternatively, it is possible that the location of the left and right knees relative to

the center of the B0 magnetic field may have had an effect (29). Previous work done in phantoms, following identical scanning acquisition parameters to the current in vivo study revealed that a phantom positioned located in the same position in relation to isocenter as the left and right knees in the current study showed little variation in relaxation times (29). This suggests to us that the differences seen in our healthy human subjects may be coming from a different source than scanner location such as different offloading times for the left and right knees. Moreover, this phantom work showed little to no variation in relaxation times of knee-sized phantoms over the time period of one week (29). Future work is needed to understand the apparent source of limb sidedness and its effect on qMRI relaxation times.

Our study had strengths and potential limitations. Important strengths of our study included investigation of visit-to-visit reliability with the subject's knee unloaded and loaded, and processing the articular cartilage of the tibia and femur with different ROIs. Not randomizing the order in which the knee was scanned provided valuable insight into the left-to-right differences in healthy subjects. Further we made every effort to control the time of day the qMRI scans were acquired, with an average of 53 minutes between the start times of visit 1 and visit 2 acquisitions. We also aimed to control the duration of off-loading of the knee prior to MRI acquisition, with an average of 3.9 minutes difference from visit 1 to visit 2. The most significant limitation of this study was the relatively small sample size. While an individual ROI may contain many voxels, more subjects would have provided more powerful insight into the referenced relationships. Last, the scanning parameters were set to ensure acquisition within the 12-minute loading window in our preliminary laboratory-based study (supplemental text) and that of Wang

et al. (24); however, longer scan times could have permitted improvements in signal-to-noise ratio and subsequent improvements in ICCs and smaller differences between left and right knees. Increased scan time will come with an increased risk of subject discomfort and motion artifact.

Conclusion

Overall, qMRI measures of T1 ρ and T2* relaxation times had fair to good reliability between visits separated at time points 7 days apart, with the tibia having higher ICC values than the femur. We observed significantly smaller differences in the mean relaxation times between visits when compared to the larger differences in mean relaxation times seen between left and right knees. Finally, while ROI selection does not seem to directly relate to ICC and mean relaxation values, it does appear to differ throughout a selection of ROIs highlighting the need for stringent methodological consideration and analysis before accurate conclusions can be made from studies of healthy and diseased populations.

References

1. Sasho T, Katsuragi J, Yamaguchi S, Haneishi H, Aizimu T, Tanaka T, Watanabe A, Sato Y, Akagi R, Matsumoto K, Uno T, Motoori K. Associations of three-dimensional T1 rho MR mapping and three-dimensional T2 mapping with macroscopic and histologic grading as a biomarker for early articular degeneration of knee cartilage. *Clin Rheumatol*. 2017 Sep;36(9):2109-2119. doi: 10.1007/s10067-017-3645-2. Epub 2017 Apr 29. PMID: 28456927.
2. Wheaton, A. J., Dodge, G. R., Elliott, D. M., Nicoll, S. B., and Reddy, R., 2005, "Quantification of Cartilage Biomechanical and Biochemical Properties via T1ρ Magnetic Resonance Imaging," *Magnetic Resonance in Medicine*, **54**(5), pp. 1087–1093.
3. Williams, A., Qian, Y., Bear, D., and Chu, C. R., 2010, "Assessing Degeneration of Human Articular Cartilage with Ultra-Short Echo Time (UTE) T2* Mapping," *Osteoarthritis Cartilage*, **18**(4), pp. 539–546.
4. Atkinson HF, Birmingham TB, Moyer RF, Yacoub D, Kanko LE, Bryant DM, Thiessen JD, Thompson RT. MRI T2 and T1ρ relaxation in patients at risk for knee osteoarthritis: a systematic review and meta-analysis. *BMC Musculoskelet Disord*. 2019 May 1;20(1):182. doi: 10.1186/s12891-019-2547-7. PMID: 31201111
5. Li X, Benjamin Ma C, Link TM, Castillo DD, Blumenkrantz G, Lozano J, Carballido-Gamio J, Ries M, Majumdar S. In vivo T(1rho) and T(2) mapping of articular cartilage in osteoarthritis of the knee using 3 T MRI. *Osteoarthritis Cartilage*. 2007 Jul;15(7):789-97. doi: 10.1016/j.joca.2007.01.011. Epub 2007 Feb 16. PMID: 17307365; PMCID: PMC2040334.31039785; PMCID: PMC6492327.
6. Yang Z, Xie C, Ou S, Zhao M, Lin Z. Cutoff points of T1 rho/T2 mapping relaxation times distinguishing early-stage and advanced osteoarthritis. *Arch Med Sci*. 2021 Aug 2;18(4):1004-1015. doi: 10.5114/aoms/140714. PMID: 35832709; PMCID: PMC9266714
7. Link TM, Joseph GB, Li X. MRI-based T_{1rho} and T₂ cartilage compositional imaging in osteoarthritis: what have we learned and what is needed to apply it clinically and in a trial setting? *Skeletal Radiol*. 2023 Nov;52(11):2137-2147. doi: 10.1007/s00256-023-04310-x. Epub 2023 Mar 31. PMID: 37000230.
8. Jerban S, Chang EY, Du J. Magnetic resonance imaging (MRI) studies of knee joint under mechanical loading: Review. *Magn Reson Imaging*. 2020 Jan;65:27-36. doi: 10.1016/j.mri.2019.09.007. Epub 2019 Oct 25. PMID: 31670237; PMCID: PMC6938531.
9. Schütz U, Martensen T, Kleiner S, Dreyhaupt J, Wegener M, Wilke HJ, Beer M. T2*-Mapping of Knee Cartilage in Response to Mechanical Loading in Alpine Skiing: A Feasibility Study. *Diagnostics (Basel)*. 2022 Jun 4;12(6):1391. doi: 10.3390/diagnostics12061391. PMID: 35741201; PMCID: PMC9222057.
10. MacKay, J. W., Low, S. B. L., Smith, T. O., Toms, A. P., McCaskie, A. W., and Gilbert, F. J., 2018, "Systematic Review and Meta-Analysis of the Reliability and Discriminative

- Validity of Cartilage Compositional MRI in Knee Osteoarthritis,” *Osteoarthritis Cartilage*, **26**(9), pp. 1140–1152.
11. Williams AA, Titchenal MR, Andriacchi TP, Chu CR. MRI UTE-T2* profile characteristics correlate to walking mechanics and patient reported outcomes 2 years after ACL reconstruction. *Osteoarthritis Cartilage*. 2018 Apr;26(4):569-579. doi: 10.1016/j.joca.2018.01.012. Epub 2018 Feb 7. PMID: 29426012; PMCID: PMC6548437.
 12. Williams AA, Titchenal MR, Do BH, Guha A, Chu CR. MRI UTE-T2* shows high incidence of cartilage subsurface matrix changes 2 years after ACL reconstruction. *J Orthop Res*. 2019 Feb;37(2):370-377. doi: 10.1002/jor.24110. Epub 2019 Jan 8. PMID: 30030866.
 13. John C Ramsdell, Bruce Beynon, Niccolo Fiorentino. “Tibial and femoral articular cartilage exhibit response to acute compressive loading in healthy knees” under review in journal of Biomechanics.
 14. Li, X., Han, E. T., Busse, R. F., and Majumdar, S., 2008, “In Vivo T1 ρ Mapping in Cartilage Using 3D Magnetization-Prepared Angle-Modulated Partitioned k-Space Spoiled Gradient Echo Snapshots (3D MAPSS),” *Magnetic Resonance in Medicine*, **59**(2), pp. 298–307.
 15. Rosset, A., Spadola, L., and Ratib, O., 2004, “OsiriX: An Open-Source Software for Navigating in Multidimensional DICOM Images,” *J Digit Imaging*, **17**(3), pp. 205–216.
 16. “GitHub - Mggardne/MRI_T1rho_T2star_reliability: Matlab Files for processing knee MRI cartilage segmentations and calculating T1rho or T2*” [Online]. Available: https://github.com/mggardne/MRI_T1rho_T2star_reliability. [Accessed: 12-Dec-2022].
 17. Klein, S., Staring, M., Murphy, K., Viergever, M. A., and Pluim, J. P. W., 2010, “Elastix: A Toolbox for Intensity-Based Medical Image Registration,” *IEEE Trans Med Imaging*, **29**(1), pp. 196–205.
 18. S. Klein, M. Staring, K. Murphy, M.A. Viergever, J.P.W. Pluim, "elastix: a toolbox for intensity based medical image registration," *IEEE Transactions on Medical Imaging*, vol. 29, no. 1, pp. 196 - 205, January 2010.
 19. D.P. Shamonin, E.E. Bron, B.P.F. Lelieveldt, M. Smits, S. Klein and M. Staring, "Fast Parallel Image Registration on CPU and GPU for Diagnostic Classification of Alzheimer's Disease", *Frontiers in Neuroinformatics*, vol. 7, no. 50, pp. 1-15, January 2014.
 20. Levenberg, K., 1944, “A Method for the Solution of Certain Non-Linear Problems in Least Squares,” *Quart. Appl. Math.*, **2**(2), pp. 164–168.
 21. Marquardt, D. W., 1963, “An Algorithm for Least-Squares Estimation of Nonlinear Parameters,” *Journal of the Society for Industrial and Applied Mathematics*, **11**(2), pp. 431–441.
 22. Zhang X, de Moura HL, Monga A, Zibetti MVW, Kijowski R, Regatte RR. Repeatability of Quantitative Knee Cartilage T₁, T₂, and T₁ ρ Mapping With 3D-MRI Fingerprinting. *J Magn Reson Imaging*. 2023 Oct 26. doi: 10.1002/jmri.29068. Epub ahead of print. PMID: 37885320.
 23. Welsch GH, Apprich S, Zbyn S, Mamisch TC, Mlynarik V, Scheffler K, Bieri O, Trattnig S. Biochemical (T₂, T₂* and magnetisation transfer ratio) MRI of knee cartilage: feasibility at ultra-high field (7T) compared with high field (3T) strength. *Eur Radiol*. 2011 Jun;21(6):1136-43. doi: 10.1007/s00330-010-2029-7. Epub 2010 Dec 12. PMID: 21153551.

24. Lartey R, Nanavati A, Kim J, Li M, Xu K, Nakamura K, Shin W, Winalski CS, Obuchowski N, Bahroos E, Link TM, Hardy PA, Peng Q, Kim J, Liu K, Fung M, Wu C, Li X. Reproducibility of $T_{1\rho}$ and T_2 quantification in a multi-vendor multi-site study. *Osteoarthritis Cartilage*. 2023 Feb;31(2):249-257. doi: 10.1016/j.joca.2022.10.017. Epub 2022 Nov 10. PMID: 36370959; PMCID: PMC10016129.
25. Li X, Han ET, Ma CB, Link TM, Newitt DC, Majumdar S. In vivo 3T spiral imaging based multi-slice $T(1\rho)$ mapping of knee cartilage in osteoarthritis. *Magn Reson Med*. 2005 Oct;54(4):929-36. doi: 10.1002/mrm.20609. PMID: 16155867.
26. Xie D, Murray J, Lartey R, Gaj S, Kim J, Li M, Eck BL, Winalski CS, Altahawi F, Jones MH, Obuchowski NA, Huston LJ, Harkins KD, Friel HT, Damon BM, Knopp MV, Kaeding CC, Spindler KP, Li X. Multi-vendor multi-site quantitative MRI analysis of cartilage degeneration 10 Years after anterior cruciate ligament reconstruction: MOON-MRI protocol and preliminary results. *Osteoarthritis Cartilage*. 2022 Dec;30(12):1647-1657. doi: 10.1016/j.joca.2022.08.006. Epub 2022 Aug 30. PMID: 36049665; PMCID: PMC9671830.
27. Wang H, Koff MF, Potter HG, Warren RF, Rodeo SA, Maher SA. An MRI-compatible loading device to assess knee joint cartilage deformation: Effect of preloading and inter-test repeatability. *J Biomech*. 2015 Sep 18;48(12):2934-40. doi: 10.1016/j.jbiomech.2015.08.006. Epub 2015 Aug 13. PMID: 26303166.
28. Van Ginckel A, Witvrouw E. Acute cartilage loading responses after an in vivo squatting exercise in people with doubtful to mild knee osteoarthritis: a case-control study. *Phys Ther*. 2013 Aug;93(8):1049-60. doi: 10.2522/ptj.20120491. Epub 2013 Apr 11. PMID: 23580627.
29. John C. Ramsdell, Bruce D. Beynnon, Andrew S. Borah, Mack G. Gardner-Morse, Jiming Zhang, Mickey I. Krug, Timothy W. Tourville, Matthew Geeslin, Mathew J. Failla, Pamela M. Vacek, Niccolo M. Fiorentino, $T_{1\rho}$ and T_2^* measurements in small and knee-sized magnetic resonance imaging phantoms: Effect of phantom size and position relative to isocenter, *Osteoarthritis Imaging*, Volume 3, Issue 3, 2023, 100162, ISSN 2772-6541, <https://doi.org/10.1016/j.ostima.2023.100162>.

Appendix A- Supplemental Materials

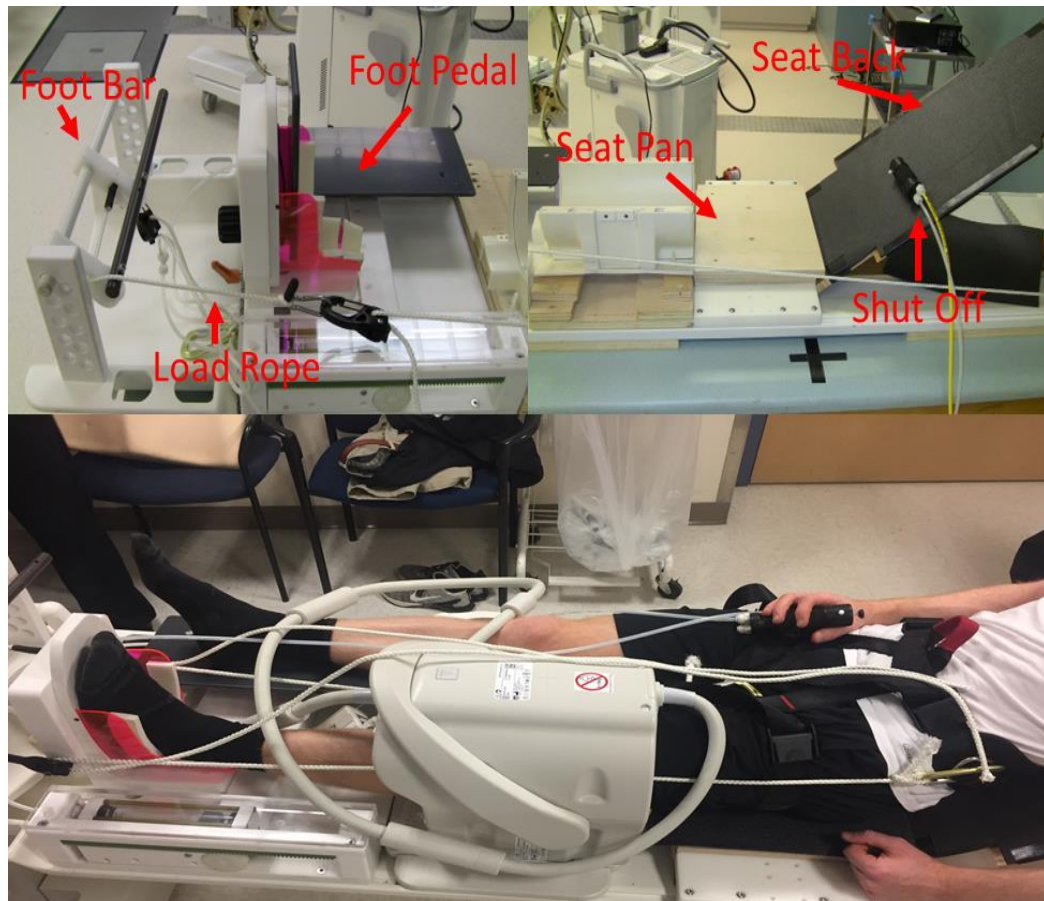


Figure S1: Illustration of the loading device developed previously and described by Ramsdell et al. [10]

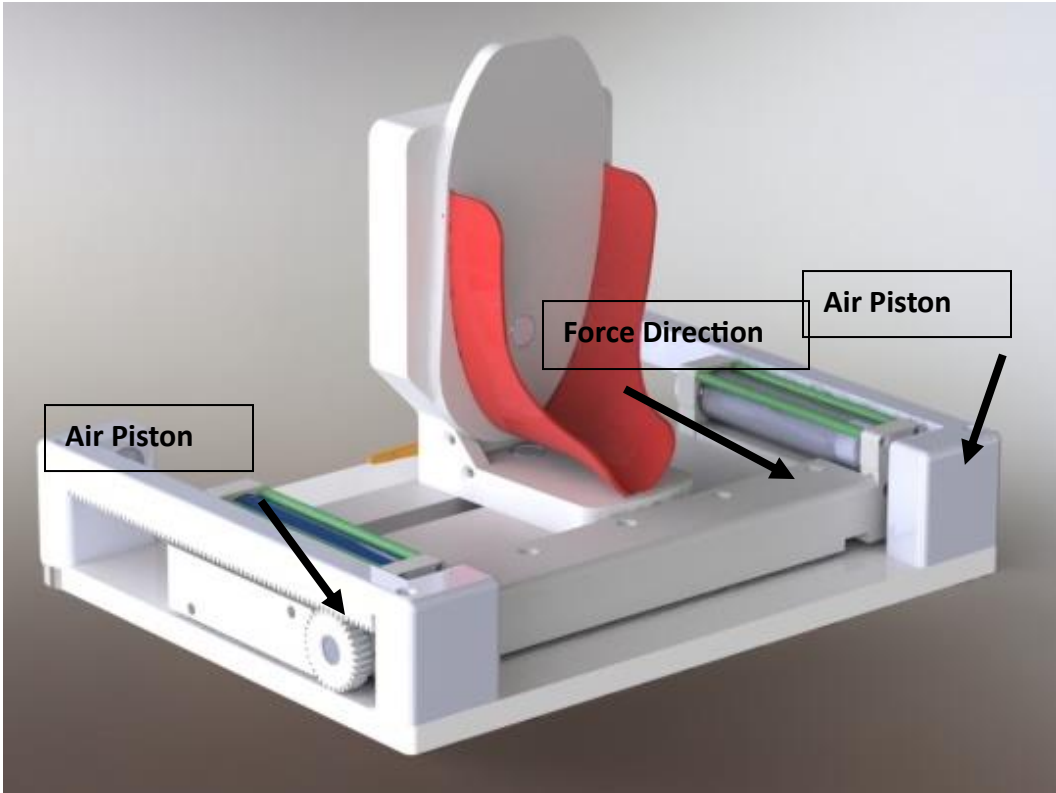


Figure S2: Illustration of the loading platform identifying the air driven pistons that apply superiorly directed force to mimic weight bearing.

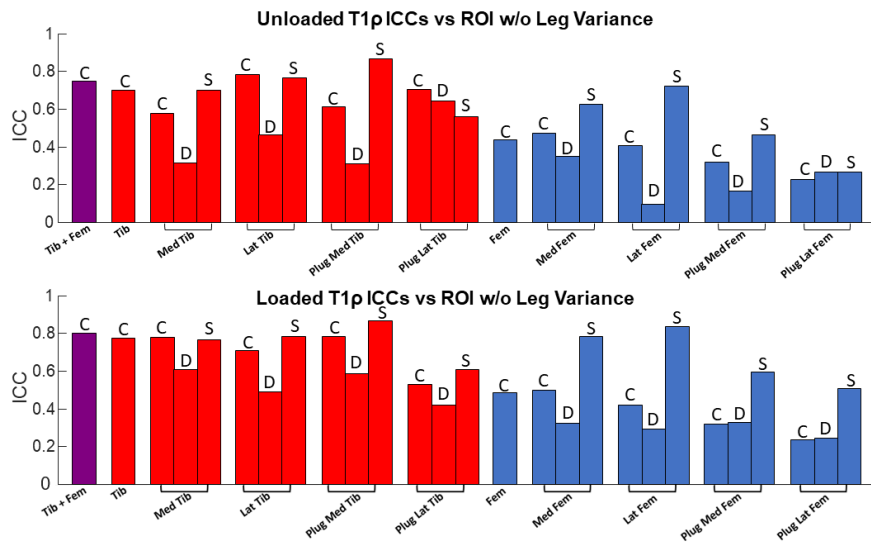


Figure S3: T1p intraclass correlation coefficients (ICCs) not including left-right leg variance for unloaded and 40% body weight loaded conditions. Letters on top of the bars signify the cartilage layer: “C” for the combined (deep and superficial) cartilage layers, “D” for the deep cartilage layer, and “S” for the superficial cartilage. Tib: tibial cartilage. Fem: femoral cartilage. Med: medial. Lat: lateral.

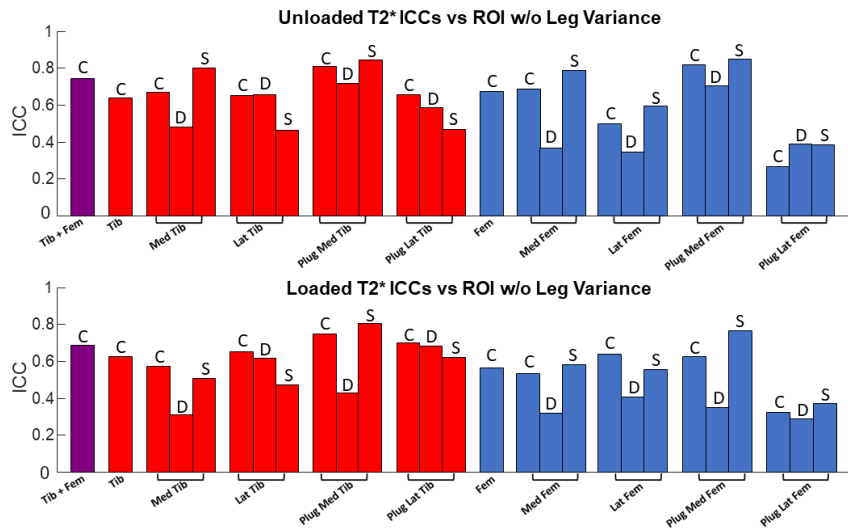


Figure S4: T2* intraclass correlation coefficients (ICCs) not including left-right leg variance for unloaded and 40% body weight loaded conditions. Letters on top of the bars signify the cartilage layer: “C” for the combined (deep and superficial) cartilage layers, “D” for the deep cartilage layer, and “S” for the superficial cartilage. Tib: tibial cartilage. Fem: femoral cartilage. Med: medial. Lat: lateral.

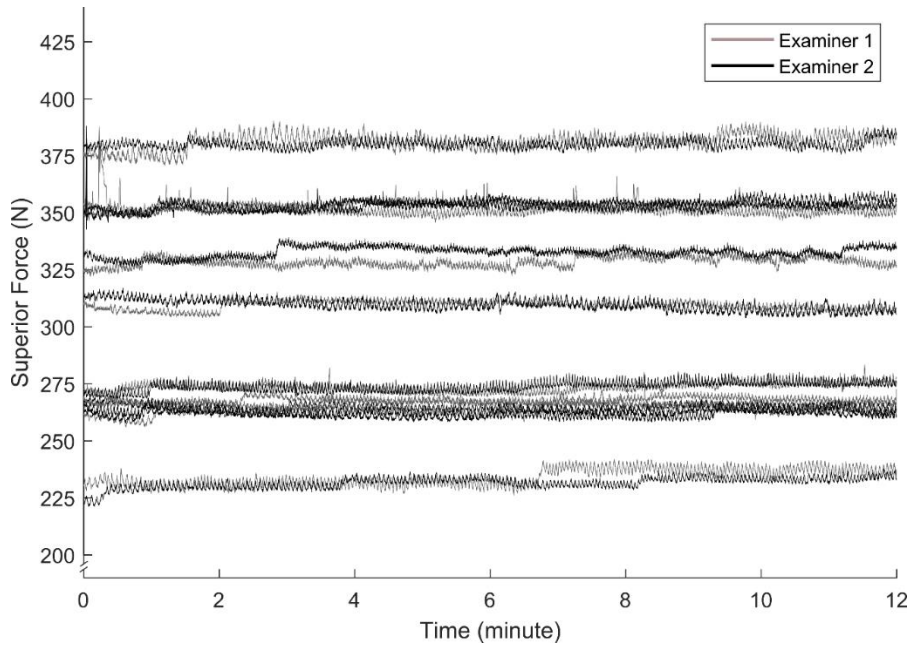


Fig. S5. Individual force profiles demonstrate small within-trial variability over the 12-minute acquisitions. For clarity, only the trial with the median force of the examiners' nine trials (three trials per day over three days) was plotted. Force profiles were plotted for Examiner 1 (gray line) and Examiner 2 (black line).

Table S1: Mean (standard deviation [SD]) T1 ρ relaxation times (ms) for visit 1 and visit 2 with no loading (See Fig. 3 for region of interest (ROI) definitions) with p-values for differences between visit 1 and visit 2. ROIs with “Deep” are the deep cartilage layer. ROIs with “Superficial” are the superficial cartilage layer. Otherwise, the ROIs are the full cartilage thickness. Significant differences ($p < .05$) shown in bold.

Region of Interest	Visit 1	Visit 2	p-value
	Mean (SD)	Mean (SD)	
Femur and Tibia	39.4 (2.9)	39.1 (2.5)	0.52
Femur	39.0 (3.7)	38.1 (3.0)	0.33
Tibia	40.5 (3.3)	41.2 (3.3)	0.24
Lateral Femur Deep	33.1 (4.0)	31.8 (3.9)	0.24
Lateral Femur Superficial	43.8 (3.9)	43.5 (3.1)	0.67
Medial Femur Deep	33.8 (4.3)	32.5 (3.7)	0.32
Medial Femur Superficial	43.8 (4.3)	43.4 (3.7)	0.66
Lateral Tibia Deep	34.2 (4.5)	36.1 (3.7)	0.08
Lateral Tibia Superficial	44.3 (3.6)	44.3 (3.2)	0.97
Medial Tibia Deep	37.9 (6.3)	39.6 (6.5)	0.44
Medial Tibia Superficial	45.6 (3.8)	44.9 (3.7)	0.32
6 mm Plug Lateral Femur	32.8 (6.5)	30.8 (6.8)	0.22
6 mm Plug Medial Femur	35.7 (7.5)	34.0 (6.3)	0.45
6 mm Plug Lateral Tibia	37.0 (4.2)	38.3 (4.2)	0.08
6 mm Plug Medial Tibia	42.4 (5.9)	43.9 (6.8)	0.32
6 mm Plug Lateral Femur Deep	26.7 (7.4)	24.0 (8.3)	0.12
6 mm Plug Lateral Femur Superficial	38.8 (6.9)	37.6 (6.0)	0.44
6 mm Plug Medial Femur Deep	27.2 (8.2)	25.2 (6.6)	0.44
6 mm Plug Medial Femur Superficial	43.9 (7.8)	42.5 (7.0)	0.48
6 mm Plug Lateral Tibia Deep	30.2 (5.9)	31.6 (5.7)	0.23
6 mm Plug Lateral Tibia Superficial	44.0 (3.8)	45.0 (3.8)	0.17
6 mm Plug Medial Tibia Deep	38.3 (8.7)	40.2 (8.6)	0.49
6 mm Plug Medial Tibia Superficial	46.7 (5.8)	47.7 (6.5)	0.20

Table S2: Mean (standard deviation [SD]) T1 ρ relaxation times (ms) for visit 1 and visit 2 loaded with 40% bodyweight (see Fig. 3 for region of interest (ROI) definitions) with p-values for differences between visit 1 and visit 2. ROIs with “Deep” are the deep cartilage layer. ROIs with “Superficial” are the superficial cartilage layer. Otherwise, the ROIs are the full cartilage thickness. Significant differences (p<.05) shown in bold.

Region of Interest	Visit 1	Visit 2	p-value
	Mean (SD)	Mean (SD)	
Femur and Tibia	40.2 (2.7)	40.1 (2.4)	0.84
Femur	40.9 (3.3)	40.6 (2.7)	0.89
Tibia	38.8 (3.5)	39.3 (4.3)	0.38
Lateral Femur Deep	36.5 (3.7)	35.5 (4.1)	0.52
Lateral Femur Superficial	45.2 (3.6)	44.7 (3.0)	0.44
Medial Femur Deep	34.5 (4.2)	35.2 (4.7)	0.63
Medial Femur Superficial	45.6 (4.4)	45.7 (3.9)	0.92
Lateral Tibia Deep	31.2 (4.5)	32.3 (5.0)	0.37
Lateral Tibia Superficial	43.7 (3.0)	44.1 (3.3)	0.27
Medial Tibia Deep	34.0 (6.4)	35.7 (7.9)	0.36
Medial Tibia Superficial	45.7 (3.8)	44.9 (4.3)	0.32
6 mm Plug Lateral Femur	37.2 (4.7)	36.8 (5.8)	0.84
6 mm Plug Medial Femur	41.2 (6.5)	39.7 (5.8)	0.62
6 mm Plug Lateral Tibia	34.4 (3.7)	35.0 (4.8)	0.42
6 mm Plug Medial Tibia	39.1 (7.0)	40.1 (7.5)	0.32
6 mm Plug Lateral Femur Deep	31.4 (6.7)	31.6 (8.8)	0.98
6 mm Plug Lateral Femur Superficial	42.9 (4.5)	41.9 (4.4)	0.52
6 mm Plug Medial Femur Deep	34.3 (8.4)	32.3 (7.8)	0.56
6 mm Plug Medial Femur Superficial	47.7 (6.8)	46.8 (6.0)	0.89
6 mm Plug Lateral Tibia Deep	27.3 (5.2)	28.5 (6.4)	0.37
6 mm Plug Lateral Tibia Superficial	41.6 (3.4)	41.5 (3.8)	0.94
6 mm Plug Medial Tibia Deep	32.3 (9.3)	35.1 (10.9)	0.20
6 mm Plug Medial Tibia Superficial	46.1 (6.3)	45.2 (6.3)	0.54

Table S3: Mean (standard deviation [SD]) T2* relaxation times (ms) for visit 1 and visit 2 with no loading (see Fig. 3 for region of interest (ROI) definitions) with p-values for differences between the left and right legs. ROIs with “Deep” are the deep cartilage layer. ROIs with “Superficial” are the superficial cartilage layer. Otherwise, the ROIs are the full cartilage thickness. Significant differences ($p < .05$) shown in bold.

Region of Interest	Visit 1	Visit 2	p-value
	Mean (SD)	Mean (SD)	
Femur and Tibia	29.1 (2.0)	29.2 (2.2)	0.72
Femur	30.4 (2.4)	31.0 (2.6)	0.30
Tibia	26.5 (1.9)	26.0 (1.9)	0.24
Lateral Femur Deep	24.7 (2.4)	25.7 (2.7)	0.29
Lateral Femur Superficial	34.6 (3.1)	35.0 (3.0)	0.53
Medial Femur Deep	26.3 (2.2)	26.9 (2.2)	0.42
Medial Femur Superficial	35.3 (4.3)	35.9 (4.3)	0.48
Lateral Tibia Deep	23.5 (3.0)	23.1 (2.9)	0.46
Lateral Tibia Superficial	32.1 (2.3)	31.7 (2.3)	0.47
Medial Tibia Deep	23.1 (2.8)	22.4 (2.4)	0.16
Medial Tibia Superficial	26.7 (2.5)	26.3 (2.9)	0.35
6 mm Plug Lateral Femur	23.9 (3.3)	25.1 (3.8)	0.28
6 mm Plug Medial Femur	30.8 (6.8)	31.5 (6.4)	0.53
6 mm Plug Lateral Tibia	23.7 (2.4)	23.6 (2.3)	0.87
6 mm Plug Medial Tibia	28.4 (4.9)	27.2 (5.2)	0.02
6 mm Plug Lateral Femur Deep	18.8 (4.2)	20.1 (4.3)	0.23
6 mm Plug Lateral Femur Superficial	29.1 (3.8)	30.1 (4.1)	0.41
6 mm Plug Medial Femur Deep	24.0 (6.4)	25.2 (4.8)	0.23
6 mm Plug Medial Femur Superficial	37.4 (8.5)	37.6 (8.9)	0.89
6 mm Plug Lateral Tibia Deep	19.3 (3.2)	18.9 (2.8)	0.50
6 mm Plug Lateral Tibia Superficial	28.0 (2.4)	28.3 (2.8)	0.66
6 mm Plug Medial Tibia Deep	24.9 (4.8)	23.8 (4.7)	0.10
6 mm Plug Medial Tibia Superficial	32.2 (5.9)	30.9 (6.5)	0.06

Table S4: Mean (standard deviation [SD]) T2* relaxation times (ms) for visit 1 and visit 2 loaded with 40% bodyweight (see Fig. 3 for region of interest (ROI) definitions) with p-values for differences between the left and right legs. ROIs with “Deep” are the deep cartilage layer. ROIs with “Superficial” are the superficial cartilage layer. Otherwise, the ROIs are the full cartilage thickness. Significant differences ($p < .05$) shown in bold.

Region of Interest	Visit 1	Visit 2	p-value
	Mean (SD)	Mean (SD)	
Femur and Tibia	31.6 (1.9)	31.1 (2.5)	0.13
Femur	34.3 (2.4)	34.0 (2.9)	0.47
Tibia	26.4 (1.9)	25.8 (2.4)	0.10
Lateral Femur Deep	32.1 (3.4)	31.6 (4.9)	0.59
Lateral Femur Superficial	35.4 (3.2)	35.2 (4.2)	0.78
Medial Femur Deep	32.0 (3.7)	31.7 (5.0)	0.82
Medial Femur Superficial	37.6 (3.6)	36.4 (5.3)	0.26
Lateral Tibia Deep	22.6 (2.8)	21.7 (3.1)	0.16
Lateral Tibia Superficial	34.0 (2.9)	32.7 (4.2)	0.14
Medial Tibia Deep	20.4 (2.3)	20.2 (2.4)	0.72
Medial Tibia Superficial	28.0 (2.2)	27.3 (3.6)	0.32
6 mm Plug Lateral Femur	33.9 (6.1)	33.5 (8.8)	0.91
6 mm Plug Medial Femur	39.3 (6.7)	39.7 (8.1)	0.77
6 mm Plug Lateral Tibia	23.6 (3.0)	22.9 (2.6)	0.16
6 mm Plug Medial Tibia	27.6 (3.4)	26.7 (4.7)	0.19
6 mm Plug Lateral Femur Deep	32.4 (10.2)	33.4 (14.0)	0.56
6 mm Plug Lateral Femur Superficial	35.5 (4.9)	34.3 (5.3)	0.48
6 mm Plug Medial Femur Deep	37.3 (8.9)	38.5 (9.7)	0.56
6 mm Plug Medial Femur Superficial	41.4 (7.6)	41.0 (9.6)	0.85
6 mm Plug Lateral Tibia Deep	18.9 (2.9)	18.5 (2.5)	0.39
6 mm Plug Lateral Tibia Superficial	28.4 (3.5)	27.5 (3.1)	0.14
6 mm Plug Medial Tibia Deep	22.6 (3.3)	22.1 (3.9)	0.52
6 mm Plug Medial Tibia Superficial	32.9 (5.2)	31.5 (6.5)	0.12

Table 1: Three-dimensional (3D) T1 ρ (A) and T2* (B) scanning parameter values.

(A) 3D T1ρ imaging		(B) 3D T2* imaging	
Parameter	Value	Parameter	Value
Field-of-view (mm ³)	250 x 141 x 96	Field-of-view (mm ³)	140 x 140 x96
Acquired matrix size	500 x 281 x 32	Acquired matrix size	232 x 232 x 24
Image orientation	Sagittal	Image orientation	Sagittal
Reconstructed matrix size	512 x 512 x 64	Reconstructed matrix size	320 x 320 x 48
Reconstructed voxel size (mm ³)	0.49 x 0.49 x 1.5	Reconstructed voxel size (mm ³)	0.44 x 0.44 x 2.00
Time of recovery (ms)	2150	Echo times (ms)	0.42, 1, 5, 15, 30
Spin-lock times (ms)	0, 10, 40, 80	Repetition time (ms)	50
Echo time (ms)	5.1	Flip angle (°)	8
Repetition time (ms)	10	Spiral acquisition window (ms)	2.9
Flip angle maximum (°)	70	Number of spiral interleaves	93
Acquisition time	9 min 11 s	Fat suppression	SPIR
Bandwidth per pixel (Hz/pix)	287.4	Acquisition duration	9 min 19 s
TFE factor	92	B ₀ shimming	PB-volume
Spin-lock frequency (Hz)	500		
Compress Sensing factor	3.2		
TFE profile order	Low-high		
TFE turbo direction	Radial		
Fat suppression	ProSet-1331		
B ₀ Shimming	PB-volume		

Table 2: Mean (standard deviation [SD]) T1 ρ relaxation times (ms) for left and right legs with no loading and loading for both full-segmentations and 6 mm plug regions of interest (ROIs, See Figure 3) with p-values for differences between the left and right legs. ROIs with “Deep” are the deep cartilage layer. ROIs with “Superficial” are the superficial cartilage layer. Otherwise, the ROIs are the full cartilage thickness. Significant differences ($p < .05$)

Region of Interest	Unloaded			Loaded			
	Left Leg Mean (SD)	Right Leg Mean (SD)	p-value	Left Leg Mean (SD)	Right Leg Mean (SD)	p-value	
Full-Surface	Lateral Femur Deep	30.8 (4.3)	34.1 (3.0)	0.03	35.3 (4.5)	36.7 (3.2)	0.26
	Lateral Femur Superficial	42.6 (3.5)	44.7 (3.2)	0.01	44.2 (3.4)	45.8 (3.0)	0.001
	Medial Femur Deep	31.6 (4.2)	34.6 (3.3)	0.01	34.0 (5.00)	35.8 (3.7)	0.19
6 mm Plug	Medial Femur Superficial	42.6 (3.9)	44.6 (3.9)	0.02	44.9 (4.0)	46.4 (4.0)	0.02
	Lateral Tibia Deep	35.1 (4.2)	35.2 (4.3)	0.90	30.7 (5.00)	32.8 (4.4)	0.14
	Lateral Tibia Superficial	42.2 (2.9)	46.4 (2.2)	<0.0001	42.9 (3.1)	44.9 (2.7)	0.01
	Medial Tibia Deep	38.9 (5.2)	38.6 (7.5)	0.85	34.6 (7.0)	35.0 (7.4)	0.82
	Medial Tibia Superficial	44.3 (3.3)	46.2 (3.9)	0.04	45.2 (4.5)	45.3 (3.6)	0.89
	Lateral Femur	28.8 (7.2)	34.8 (4.5)	0.01	35.8 (6.1)	38.1 (4.0)	0.18
6 mm Plug	Medial Femur	32.2 (6.9)	37.6 (6.0)	0.001	38.1 (7.0)	42.6 (4.4)	0.03
	Lateral Tibia	36.8 (3.8)	38.5 (4.5)	0.09	34.0 (4.3)	35.3 (4.1)	0.28
	Medial Tibia	41.9 (5.0)	44.4 (7.4)	0.09	38.3 (6.9)	40.9 (7.4)	0.046
	Lateral Femur Deep	22.6 (8.8)	28.3 (5.8)	0.04	31.0 (9.9)	32.0 (5.2)	0.73
	Lateral Femur Superficial	35.2 (6.4)	41.2 (4.9)	0.001	40.6 (4.3)	44.1 (3.8)	0.01
	Medial Femur Deep	23.5 (7.6)	28.9 (6.3)	0.02	31.5 (10.0)	35.0 (5.2)	0.18
	Medial Femur Superficial	40.4 (7.0)	45.9 (6.7)	0.01	44.4 (6.0)	49.9 (5.5)	0.001
	Lateral Tibia Deep	31.1 (5.4)	30.7 (6.3)	0.74	27.5 (6.3)	28.3 (5.4)	0.55
	Lateral Tibia Superficial	42.6 (3.0)	46.5 (3.5)	0.001	40.6 (3.3)	42.4 (3.6)	0.10
	Medial Tibia Deep	38.8 (6.8)	39.7 (10.2)	0.65	32.6 (9.6)	34.8 (10.7)	0.41
	Medial Tibia Superficial	45.2 (5.2)	49.2 (6.4)	0.002	44.0 (6.5)	47.2 (5.7)	0.002

Table 3: Mean (standard deviation [SD]) T2* relaxation times (ms) for left and right legs with no loading and loading for both full-segmentations and 6 mm plug regions of interest (ROIs. See Figure 3) with p-values for differences between the left and right legs. ROIs with "Deep" are the deep cartilage layer. ROIs with "Superficial" are the superficial cartilage layer. Otherwise, the ROIs are the full cartilage thickness. Significant differences ($p < .05$) shown in bold.

Region of Interest	Unloaded		p-value	Loaded		
	Left Leg Mean (SD)	Right leg Mean (SD)		Left leg Mean (SD)	Right leg Mean (SD)	
Femur and Tibia	28.6 (1.9)	29.7 (2.2)	0.01	30.5 (2.0)	32.3 (2.1)	0.002
Femur	30.2 (2.3)	31.2 (2.7)	0.051	33.1 (2.4)	35.4 (2.4)	0.004
Tibia	25.6 (1.4)	26.9 (2.1)	0.01	25.6 (1.9)	26.7 (2.3)	0.12
Full-Surface						
Lateral Femur Deep	24.4 (2.1)	26.0 (2.8)	0.01	29.8 (3.2)	33.9 (4.1)	0.002
Lateral Femur Superficial	33.9 (3.0)	35.7 (2.7)	0.06	34.5 (3.2)	36.0 (4.1)	0.12
Medial Femur Deep	26.6 (1.9)	26.7 (2.5)	0.82	30.9 (4.0)	32.8 (4.6)	0.08
Medial Femur Superficial	35.2 (3.8)	36.0 (4.7)	0.38	36.4 (4.2)	37.6 (4.8)	0.29
Lateral Tibia Deep	22.5 (2.6)	24.2 (3.0)	0.004	21.9 (3.0)	22.4 (2.9)	0.42
Lateral Tibia Superficial	31.1 (2.1)	32.7 (2.3)	0.03	32.6 (2.8)	34.1 (4.3)	0.17
Medial Tibia Deep	22.0 (2.2)	23.5 (2.8)	0.06	20.6 (2.2)	20.2 (2.5)	0.55
Medial Tibia Superficial	26.1 (2.6)	26.8 (2.8)	0.15	27.1 (2.5)	28.3 (3.4)	0.16
6mm Plug						
Lateral Femur	23.5 (2.7)	25.6 (4.0)	0.02	30.5 (5.5)	37.2 (7.8)	0.02
Medial Femur	30.6 (6.8)	31.7 (6.4)	0.21	37.4 (7.2)	41.8 (6.9)	0.02
Lateral Tibia	22.9 (2.0)	24.4 (2.4)	0.02	22.9 (3.0)	23.7 (2.6)	0.41
Medial Tibia	26.6 (4.1)	29.1 (5.6)	0.03	26.3 (4.1)	28.1 (3.9)	0.06
Lateral Femur Deep	18.2 (3.1)	20.8 (4.9)	0.04	28.1 (10.1)	28.1 (10.1)	0.03
Lateral Femur Superficial	28.8 (3.5)	30.4 (4.3)	0.10	33.4 (3.7)	36.6 (5.9)	0.08
Medial Femur Deep	24.6 (6.0)	24.6 (5.2)	0.99	35.7 (9.0)	40.3 (9.0)	0.09
Medial Femur Superficial	36.3 (8.4)	38.7 (8.8)	0.04	39.2 (7.8)	43.5 (8.9)	0.04
Lateral Tibia Deep	18.2 (2.4)	20.0 (3.3)	0.03	18.4 (2.9)	19.1 (2.5)	0.29
Lateral Tibia Superficial	27.6 (2.3)	28.8 (2.8)	0.11	27.6 (3.4)	28.4 (3.2)	0.59
Medial Tibia Deep	23.2 (4.0)	25.5 (5.2)	0.04	22.2 (4.0)	22.5 (3.1)	0.92
Medial Tibia Superficial	30.2 (5.3)	32.8 (6.8)	0.04	30.7 (5.2)	33.9 (6.2)	0.02